Exp. Theo. NANOTECHNOLOGY 10 (2026) 1365-1378 https://doi.org/10.56053/10.3.1365

Laser ablation synthesized ZnO, CuO and ZnO:CuO nanomaterials: A comparative study of structural, optical and antibacterial performance

Rifqa Amer Salman[1], Gheyath imad mohammed[2], Zahraa Qasim mahdi[3,], Salwa ghali badiwi[4], Fatimatulzahraa withaq aswad[5]*

[1]Al-Iraqia University, Baghdad, Iraq
[2]Department of Science, College of Basic Education, University of Wasit, Wasit, Iraq
[3]Department of Chemistry, College of Science, University of Baghdad, Baghdad, Iraq
[4]Quality Assurance and Performance Evaluation Department, Mustansiriyah University, Baghdad, Iraq
[5] Department of internal and preventive veterinary medicine, college of veterinary medicine, Baghdad University, Baghdad, Iraq
[*]) Email: Zahraa.q@sc.uobaghdad.edu.iq

Received 21/4/2026, *Received in revised form* 1/5/2026, *Accepted* 16/6/2026, *Published* 15/7/2026

The synthesis of ZnO and CuO as well as ZnO:CuO nanoscale, is described in this paper using the laser ablation method. X-ray diffraction (XRD), scanning electron microscopy (SEM), atomic force microscopy (AFM), and UV-Vis spectroscopy were applied to validate the characterization performed on the produced ZnO, CuO, and ZnO:CuO nanoparticles. The XRD characteristics show that ZnO diffraction peaks were detected at 2θ angles of 31.55°, 34.19°, 36.03°, 56.42°, and 62.80° as well, which can be interpreted as a hexagonal wurtzite structure. On the other hand, CuO had peaks at 35.39°, 38.71°, 48.33°, and 61.50°, which confirmed the presence of a monoclinic structure. The ZnO:CuO nanocomposite exhibited peaks originating from both materials, indicating the proper integration of CuO into its structure. For CuO, elevated strain due to lattice distortion also came during the analysis, meaning ZnO had a significantly lower strain compared with CuO, pointing to better structure stability. With AFM results, we found out that ZnO films had an average grain size of 67.74 nm and surface roughness (Ra) of 2.572 nm, while CuO films had a larger average grain size of 85.65 nm and a Ra of 43.27 nm. Compared with the ZnO:CuO composite, the grain size was decreased to 39.29 nm, and the roughness increased to a Ra of 42.26 nm. According to the optical properties, ZnO

bands have a band gap of 3.18 eV, CuO has a narrower 2.76 eV band gap, and this composite has a band gap of 2.98 eV with intermediate separation. Antimicrobial studies revealed that ZnO:CuO was successful against Gram-positive bacteria, and CuO had the best activity against Gram-negative bacteria.

Keywords: ZnO:CuO; Nanostructures; Optical; Structural; Antibacterial.

1. INTRODUCTION

Recently, metal and metal oxide nanoparticles have attracted attention for their improved properties and have been applied in multiple fields [1,2]. Zinc oxide (ZnO) and copper oxide (CuO) nanoparticles are the focus of this study due to their distinctive physicochemical and biological properties, which render them highly useful for multifunctional applications [3,4]. ZnO nanoparticles have been known to possess a wide band gap [5], high exciton binding energy [6], chemical stability [7], and high biocompatibility [8], and are reported to be able to improve optical characteristics and antibacterial activity [9]. Conversely, CuO nanoparticles show remarkable catalytic activity [10], a narrow band gap [11], and strong antimicrobial properties that correspond with copper ion release and ROS generation [12]. A wide variety of nanoparticles made of a variety of materials have been prepared physically and chemically. Techniques to prepare these nanoparticles include the use of pulsed laser deposition [13,14], sol-gel synthesis [15], chemical coprecipitation [16], thermal decomposition [17], and plasma jet [18]. Laser ablation has recently been a popular green method for the synthesis of nanomaterials owing to its simple procedures, high purity, and green environment [19]. This method does not include chemical precursors or stabilizers and is great for nanoparticles free of contaminants [20]. More specifically, pulsed laser ablation in liquids (PLAL) has demonstrated to be an efficient method for the material and technique for fabricating metal oxide nanoparticles with fine control of the size and shape. The interaction of the laser with the material produces fast heating, plasma formation, and cool down with great energy pulse, finally leading to the generation of nanoparticles with distinct structure and optical characteristics [21,22]. Compared to the individual components, incorporating ZnO and CuO in a hybrid nanostructure enhances antibacterial performance [23]. As a result, ZnO:CuO nanocomposites emerge as a promising choice for advanced applications, particularly in antibacterial treatments and environmental remediation. Herein, we employ the laser ablation technique to fabricate ZnO, CuO, and ZnO–CuO nanocomposites while examining their structural and optical properties. Also, the antibacterial activity of the prepared nanomaterials is evaluated against both Gram-positive and Gram-negative bacteria.

2. EXPERIMENTAL

Nanoparticles of ZnO and CuO were prepared via PLAL. Targets made of Zn and Cu metals were placed in 2 mL of distilled water with the water level adjusted to about 10 mm above the surface of the targets. Nd: YAG laser with a wavelength of 1064 nm was chosen for the laser ablation. The wavelength was provided with 400 mJ of energy during ablation. The Nd: YAG lasers used a repetition frequency of 7 Hz, with a pulse duration of 10 ns. The copper and zinc nanoparticles were combined in equal amounts, and a uniform mixture was achieved using ultrasonication. The effectiveness of these nanoparticles against both Gram-positive and Gram-negative bacteria was evaluated. For studying their structural and optical properties, they were applied to glass using the spin coating technique. The experimental setup is shown in Figure 1.

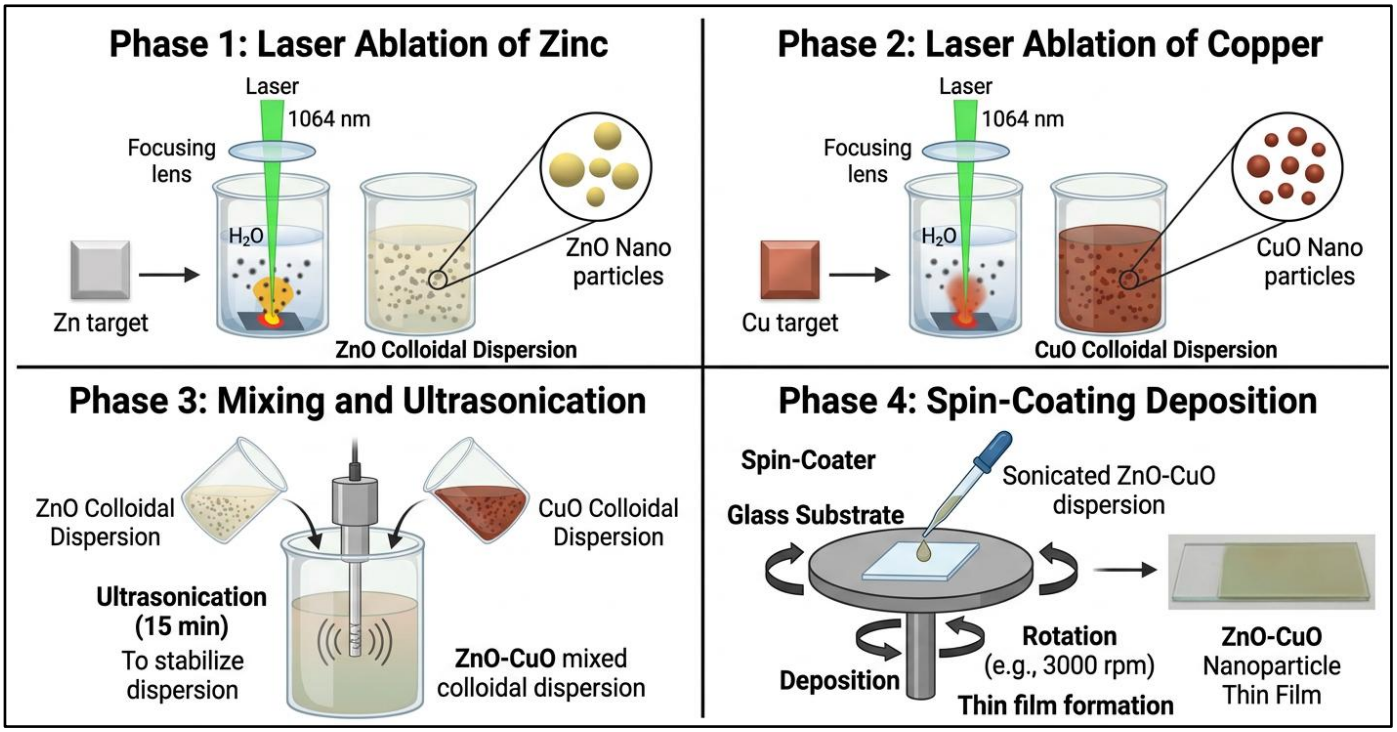

Figure 1 The working method used to form pure oxide nanoparticles from zinc and copper metals and a mixture of them.

3. RESULTS AND DISCUSSION

3.1. XRD

The X-ray diffraction (XRD) patterns of ZnO, CuO, and ZnO: CuO nanostructures are presented in Figures 2-5, respectively. The diffraction peaks which are generated for ZnO at the 2θ angles 31.55°, 34.19°, 36.03°, 56.42°, and 62.80° correspond to the (100), (002), (101), (110), and (103) crystal planes respectively, confirming the creation of a hexagonal wurtzite structure corresponding to the standard reference data (JCPDS card No. 96-901-1663) [24,25]. Sharp, high-intensity peaks indicate that the synthesized ZnO nanoparticles exhibit good crystallinity [26]. For CuO, the diffraction peaks at 35.39°, 38.71°, 48.33°, and 61.50° correspond to the (−111), (111), (−202), and (−113) planes, respectively, confirming the monoclinic nature of CuO [27,28]. Relative to ZnO, the peaks are broader, indicating smaller crystallite sizes and more widespread lattice distortion [29]. With respect to the ZnO:CuO nanocomposite, the observation of diffraction peaks for the ZnO and CuO phases confirms the formation of a hybrid nanostructure with no appearances of impurity phases [30]. The presence of both phases implies an efficient incorporation of CuO into the ZnO matrix and may contribute to improving the structural and functional properties of the composite material. The crystallite size (D) was determined according to Scherrer's equation [31]:

$$D = \frac{0.9\lambda}{\beta cos\theta} \quad (1)$$

where λ is the X-ray wavelength and β represents the FWHM of the diffraction peak. For ZnO, the calculated crystallite size ranged from 21.3 to 33.7 nm, which suggests relatively large and unique grains. In contrast, the crystallite sizes of CuO, located between 7.1 and 14.1 nm, were smaller, confirming the peak range broadening. For ZnO: CuO composite, values for the crystallite size indicated that the bigger ZnO grain and smaller CuO particle coexist, indicating that both particles are

present due to the material being composite-type [32]. The strain value (ε), reflecting lattice distortion, was deduced through [33]

$$\varepsilon = \frac{\beta cos\theta}{4} \quad (2)$$

The results indicate that ZnO has smaller strain values to those of CuO, which suggests better structural stability. CuO presents higher strain owing to a smaller crystallite size and distortion of the lattice [34]. However, we note that in the case of the ZnO: CuO composite, the applied strain values indicate a mild relaxation of internal stress, in comparison to pure CuO, potentially owing to the stabilizing effect of ZnO. All information, such as the crystallite size and the strain, is given in Table 1 in a summarized structural parameter.

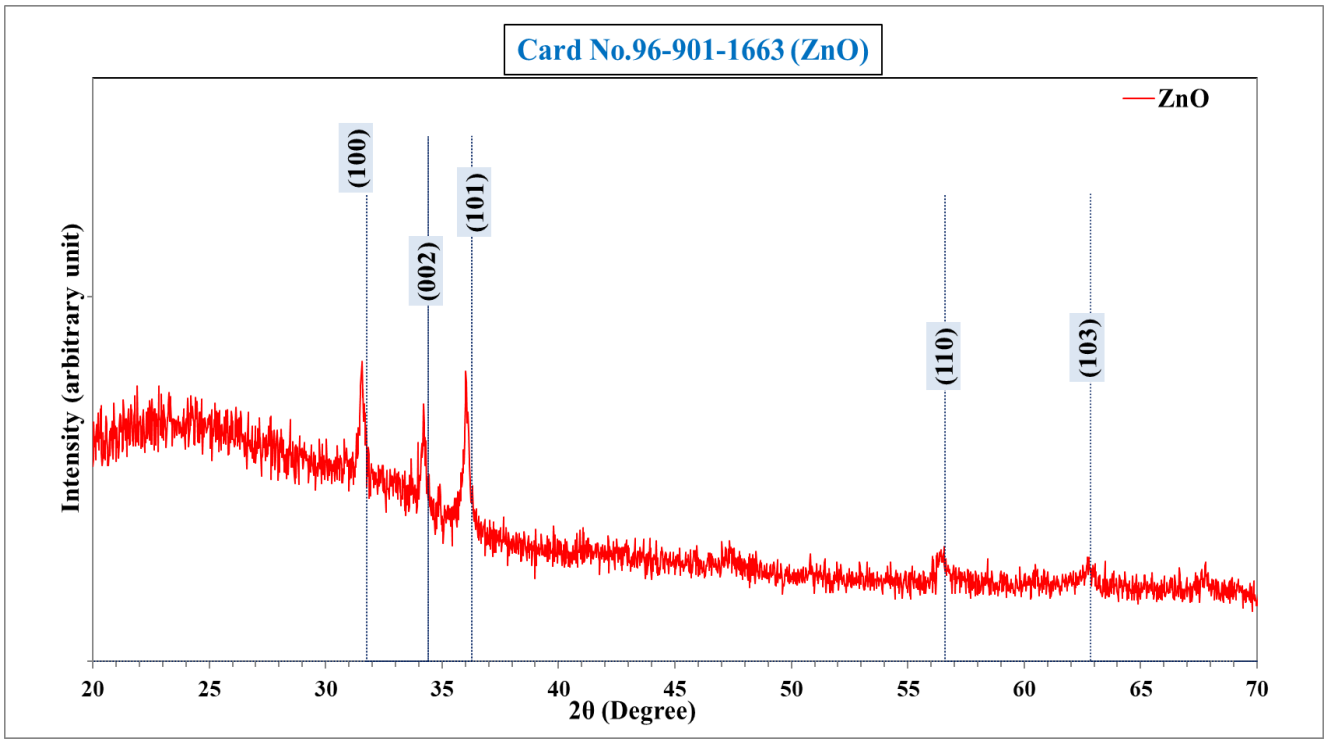

Figure 2 XRD pattern for ZnO thin film.

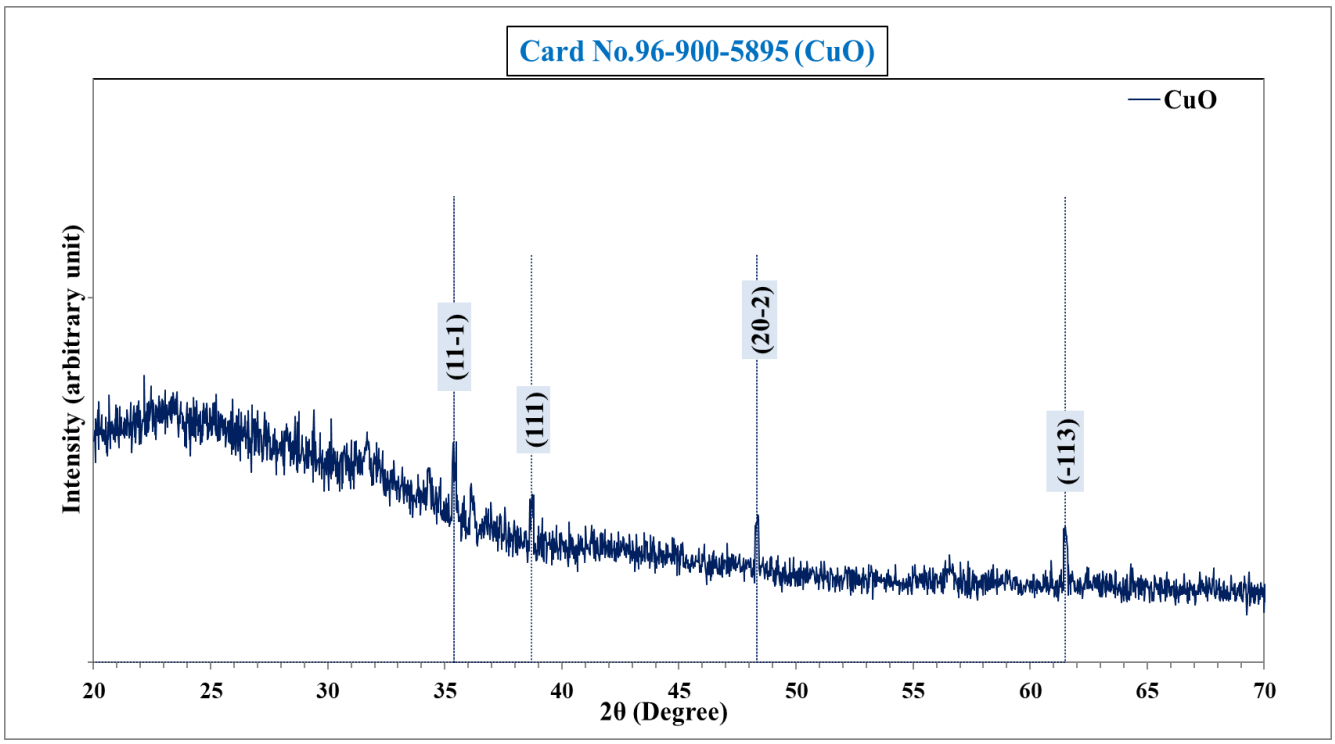

Figure 3 XRD pattern for CuO thin film.

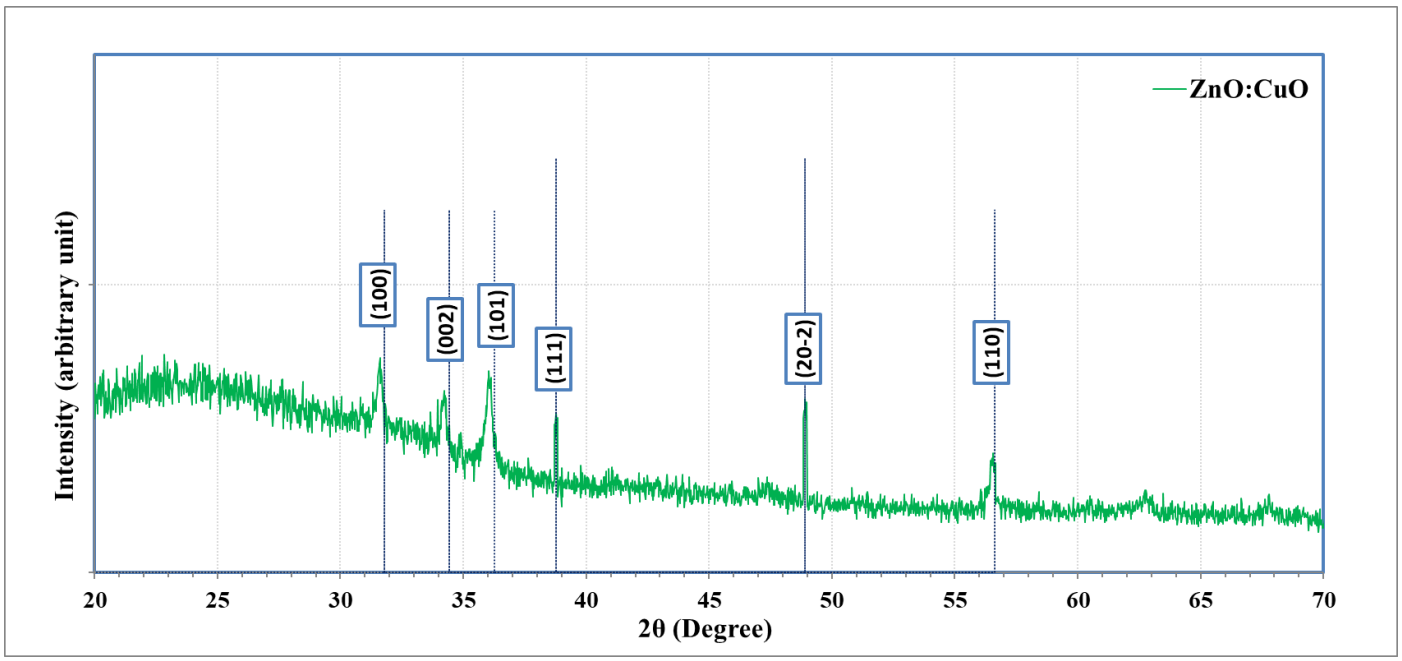

Figure 4 XRD pattern for ZnO: CuO thin film.

Table 1 Structural properties of ZnO, CuO, and ZnO: CuO.

Sample	2θ (Deg.)	FWHM (Deg.)	d_{hkl} Exp. (Å)	d_{hkl} Std. (Å)	D (nm)	hkl	Phase	Strain (ε)
ZnO	31.5561	0.2819	2.8329	2.8137	29.3	(100)	Hex. ZnO	0.00118
	34.1985	0.2466	2.6198	2.6035	33.7	(002)	Hex. ZnO	0.00103
	36.0305	0.2819	2.4907	2.4754	29.6	(101)	Hex. ZnO	0.00117
	56.4298	0.4228	1.6293	1.6245	21.3	(110)	Hex. ZnO	0.00173
	62.8068	0.3170	1.4783	1.4772	29.4	(103)	Hex. ZnO	0.00127
CuO	35.3936	0.6123	2.5340	2.523	13.6	(11-1)	Mono. CuO	0.00253
	38.7172	1.1807	2.3238	2.315	7.1	(111)	Mono. CuO	0.00483
	48.3382	0.7434	1.8814	1.875	11.7	(20-2)	Mono. CuO	0.0029
	61.5015	0.6560	1.5065	1.505	14.1	(-113)	Mon. CuO	0.00246
ZnO:CuO	31.5561	0.2819	2.8329	2.8137	29.3	(100)	ZnO	0.00118
	34.1985	0.2466	2.6198	2.6035	33.7	(002)	ZnO	0.00103
	36.0305	0.2819	2.4907	2.4754	29.6	(101)	ZnO	0.00117
	38.7789	0.8000	2.3203	2.315	10.5	(111)	CuO	0.00329
	48.9263	0.8842	1.8601	1.875	9.9	(20-2)	CuO	0.00345
	56.6100	0.3170	1.6245	1.6245	28.5	(110)	ZnO	0.00129

3.2. AFM

Figure 5 (a–c) shows the AFM micrographs in conjunction with the surface roughness assessment for ZnO, CuO, and ZnO:CuO thin films. The three-dimensional surface morphology shows a notable difference in grain distribution and surface features among the samples. ZnO film, on the other hand, displays relatively smooth, uniform nanograins at an average particle size of 67.74 nm and very low surface roughness values (Ra = 2.572 nm and RMS = 3.296 nm) (as shown in Table 2), which are indications of an even surface [35]. The CuO film, however, shows a rougher surface with larger grain structure (85.65 nm), which is evidenced by the higher roughness measurements (Ra = 43.27 nm and RMS = 55.40 nm). Such an increase suggests more pronounced surface irregularities and grain clustering [36]. A distinct reduction in particle size (39.29 nm) was obtained for the ZnO:CuO composite; ZnO application shows suppression of grain expansion as opposed to the individual oxides.

While the grain size decreases, surface roughness is still relatively high (Ra = 42.26 nm and RMS = 55.92 nm), suggesting that the composite leads to non-uniformity at the surface due to phase interactions. The results indicate that although ZnO contributed to decreasing grain size in the composite, CuO's influence dominates surface roughness. All the AFM parameters collected are listed in Table 2.

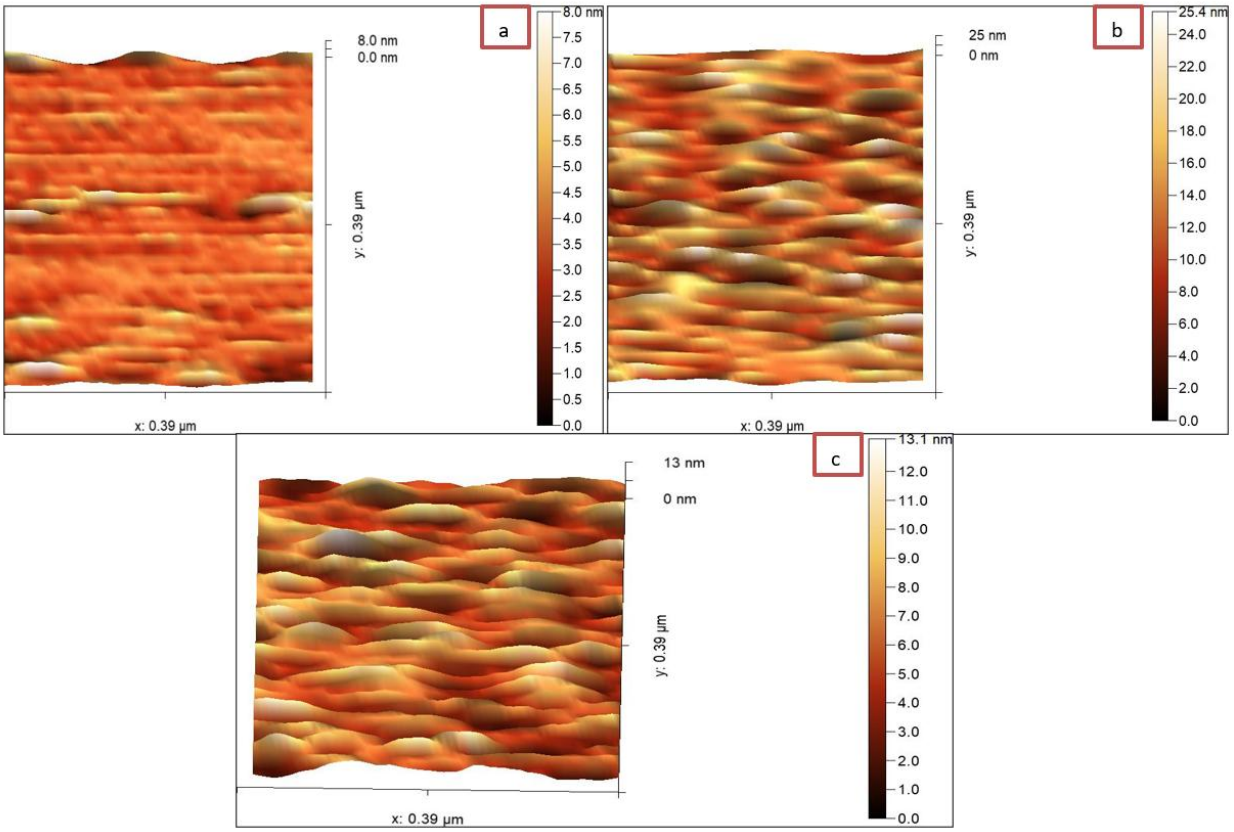

Figure 5 AFM image for (a) ZnO, (b) CuO, (c) ZnO: CuO thin film.

Table 2 AFM parameter for ZnO, CuO, and ZnO: CuO thin film.

Element	Root mean square (RMS) (nm)	Average surface roughness (nm)	Average particle diameter (nm)
ZnO	3.296	2.572	67.74
CuO	55.40	43.27	85.65
ZnO: CuO	55.92	42.26	39.29

3.3. SEM

Figure 6 (a–c) SEM images for the ZnO, CuO, and ZnO: CuO samples, respectively, are presented. The surface of ZnO seems fairly homogeneous, with even and close particles on the surface, indicating good surface coverage. The CuO sample presents a rough and irregular morphology with a large number of clumping particles and bigger aggregates, which indicates an uneven surface structure. The

ZnO: CuO composite has better particle distribution than CuO, exhibiting smaller and more dispersed grains. However, some agglomeration can still be observed, indicating interactions between ZnO and CuO phases. The results suggest ZnO contributed to increasing the uniformity of the composite surface, and CuO played a role in the increased surface roughness and aggregated particle structure.

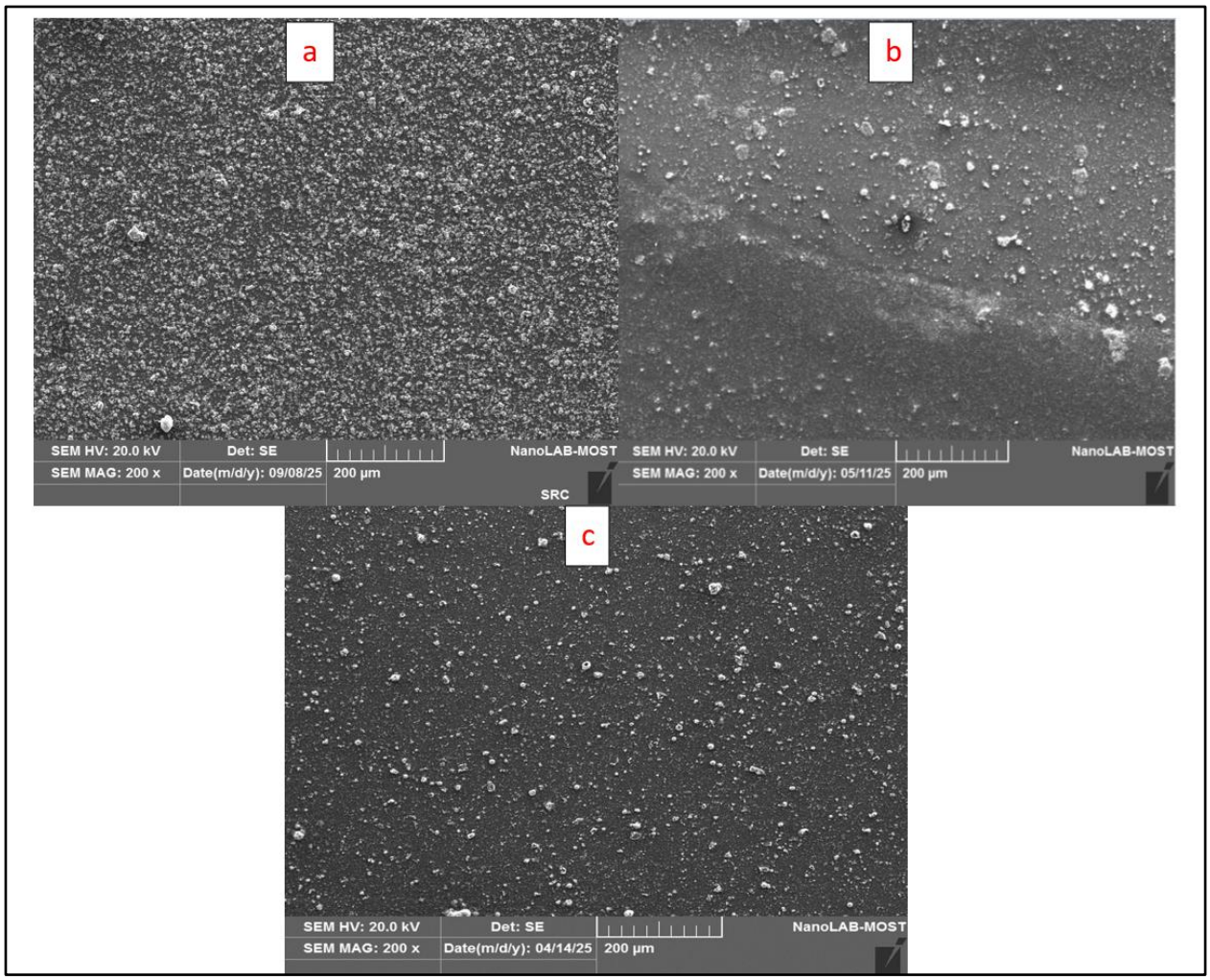

Figure 6 SEM image for (a) ZnO, (b) CuO, (c) ZnO: CuO thin film.

3.4. Optical properties

Absorbance spectra and Tauc plots of samples ZnO, CuO and ZnO:CuO are shown in Figures 7, 8 and 9 (a–b). All samples exhibit an absorbance profile that is significant in the UV range (350–400 nm) before the absorption shifts to the visible spectral range. The bandgap energy E_g of the films can be estimated using Tauc's relation [37]:

$$(\alpha hv)^2 = A\,(hv - E_g) \quad (3)$$

Where A is a constant, hv is the photon energy, and α is the absorption coefficient. ZnO has a lower absorption value (0.90–0.12 a.u), and has a clear absorption edge (between 350 and 380 nm), indicating a wide band gap of 3.18 eV typical of the transparent semiconductor properties [38]. Whereas CuO (1.20–0.25 a.u) has higher absorbance and has a broader absorption range (350–400 nm). This contributes to light absorption improvement and a narrow band gap of 2.76 eV, attributed both to intrinsic p-type properties and higher defect states [39]. The absorbance of ZnO: CuO

composite is intermediate between ZnO and CuO (1.05–0.17 a.u) with an absorption edge in (350–390 nm). The band gap is reduced to 2.98 eV when compared to ZnO, which would imply the intermediate energy levels generated due to the ZnO and CuO phases interacting [40]. Reduction of band gap in the composite facilitates light absorption; it is also advantageous in photocatalysis and antibacterial applications [41-45].

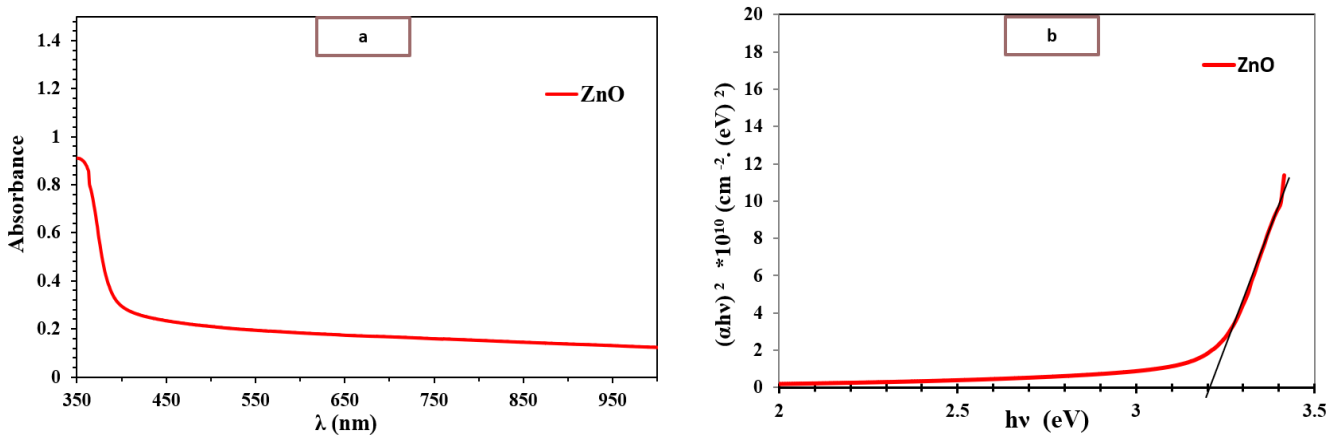

Figure 7 Absorbance and Optical band gap energy for ZnO thin film**.**

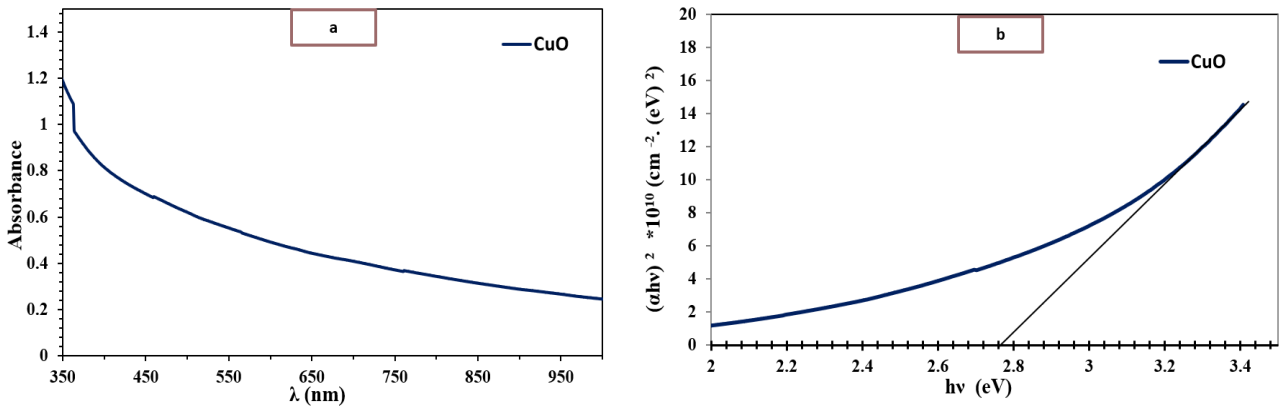

Figure 8 Absorbance and Optical band gap energy for CuO thin film

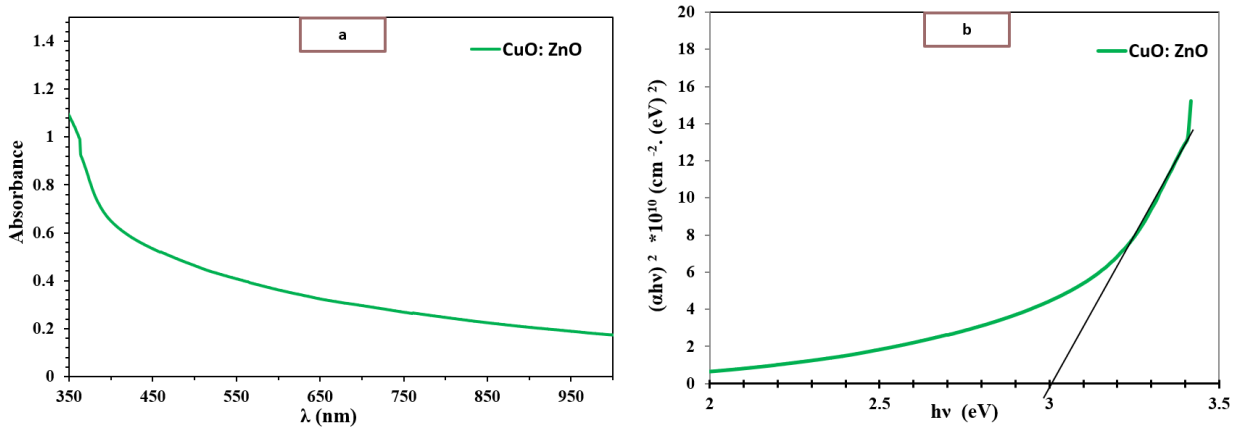

Figure 9 Absorbance and Optical band gap energy for ZnO: CuO thin film.

3.5. Antibacterial Performance

Figure 10 clearly shows the inhibition zones of ZnO, CuO, and ZnO: CuO on different bacterial strains determined using agar diffusion assay. The visualization in Figure 10 verifies that the inhibition zones are visible around the samples, thus indicating that the antibacterial effect is high [46, 47].

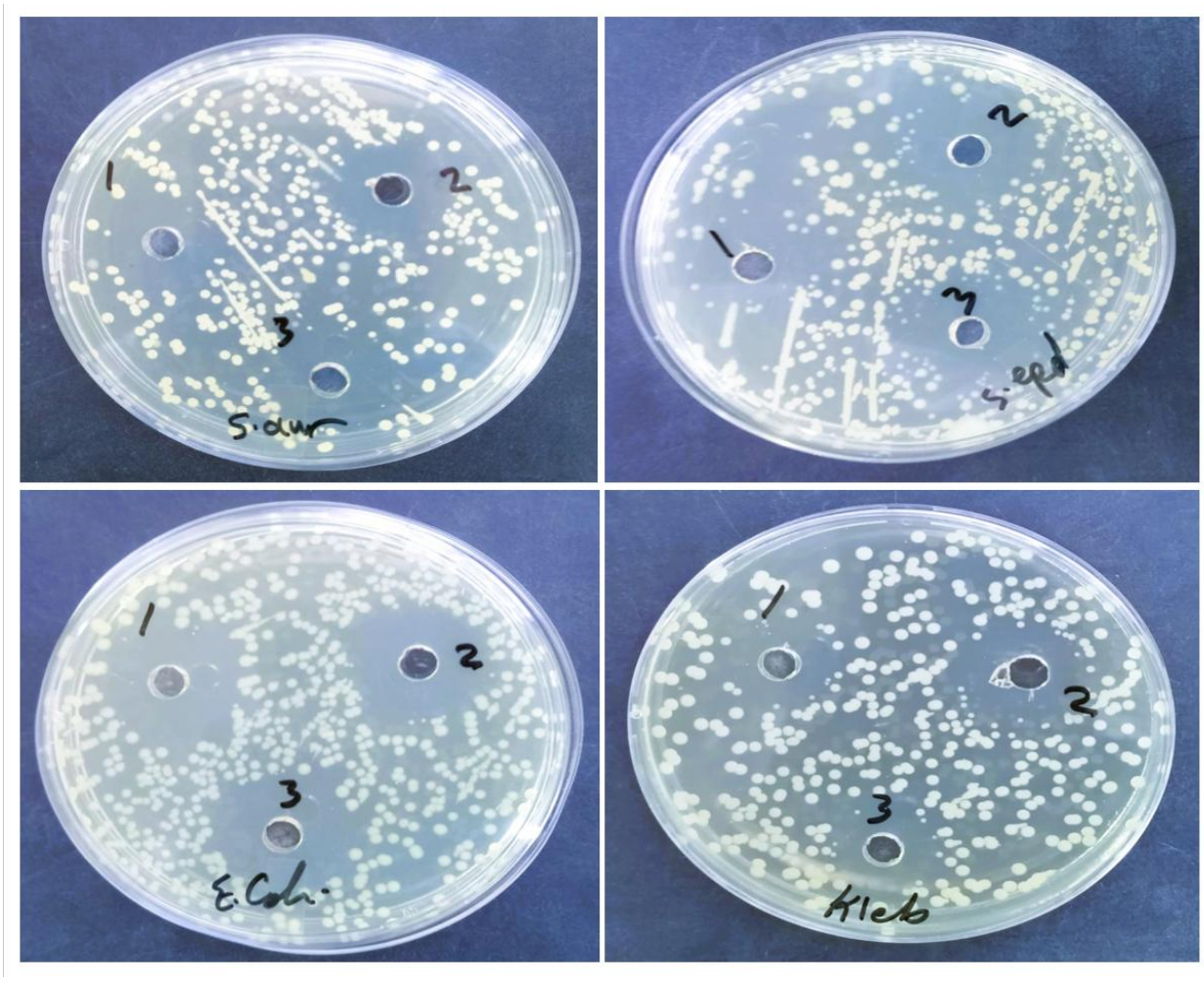

Figure 10 Inhibition zone in mm for activity of (1) ZnO, (2) CuO, (3) ZnO: CuO.

This comparison is supported by quantitative data available in both Table 3 and Figure 11, supporting the discovery that the ZnO:CuO composite shows the highest efficacy against Gram-positive bacteria (S. aureus and S. epidermidis) with an average observation of 25.5 ± 0.71 mm, whereas ZnO and CuO measurement were both 23.5 mm. This enhancement is associated with the synergistic effect between ZnO and CuO which increases reactive oxygen species (ROS) generation and induces damage to the cell wall [48, 49]. In contrast, for Gram-negative bacteria (E. coli and Klebsiella), CuO has the highest antibacterial effectiveness (23.5 ± 2.12 mm), followed by ZnO (21.0 ± 0.00 mm). On the contrary, the ZnO: CuO composite showed reduced activity (19.5 ± 3.54 mm) as shown in Table 3 and Figure 12 (bar graph with standard deviation) [50].

Table 3 Mean and standard deviation for positive and negative bacteria.

Category	Sample	S. aureus	S.epd	E. coli	Kleb	Mean ± SD
Gram-positive	ZnO	22	25	—	—	23.5 ± 2.12
	CuO	23	24	—	—	23.5 ± 0.71
	ZnO: CuO	26	25	—	—	**25.5 ± 0.71**
Gram-negative	ZnO	—	—	21	21	21.0 ± 0.00
	CuO	—	—	25	22	23.5 ± 2.12
	ZnO: CuO	—	—	22	17	19.5 ± 3.54

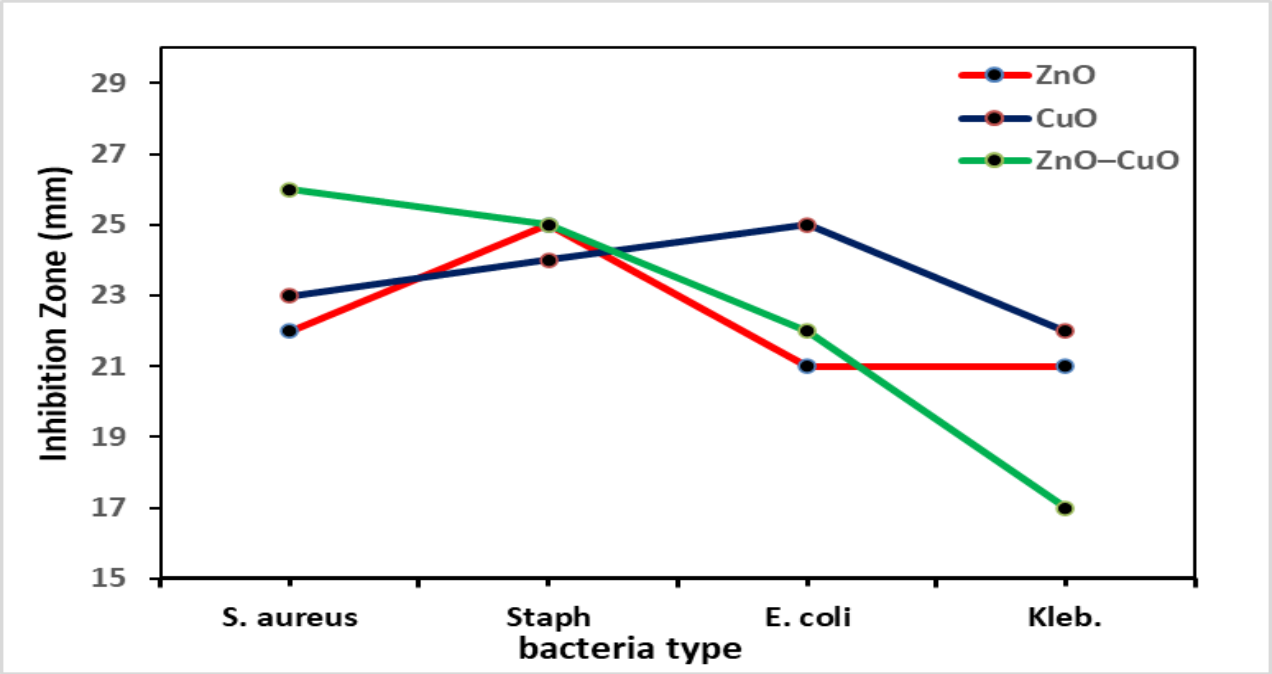

Figure 11 Line graph for the relation between type of bacteria and inhibition zone.

This behavior can be explained by the structural differences in bacterial cell walls. Gram-negative bacteria possess an outer membrane that limits nanoparticle penetration, and the increased surface roughness and aggregation in the composite (as confirmed by AFM and SEM) may reduce its effective interaction with bacterial cells [41,42]. Meanwhile, Gram-positive bacteria, having a simpler cell wall structure, are more susceptible to the combined effects of ZnO and CuO [43,44]. The results indicate that the ZnO:CuO composite is more effective against Gram-positive bacteria, while CuO alone shows better performance against Gram-negative strains.

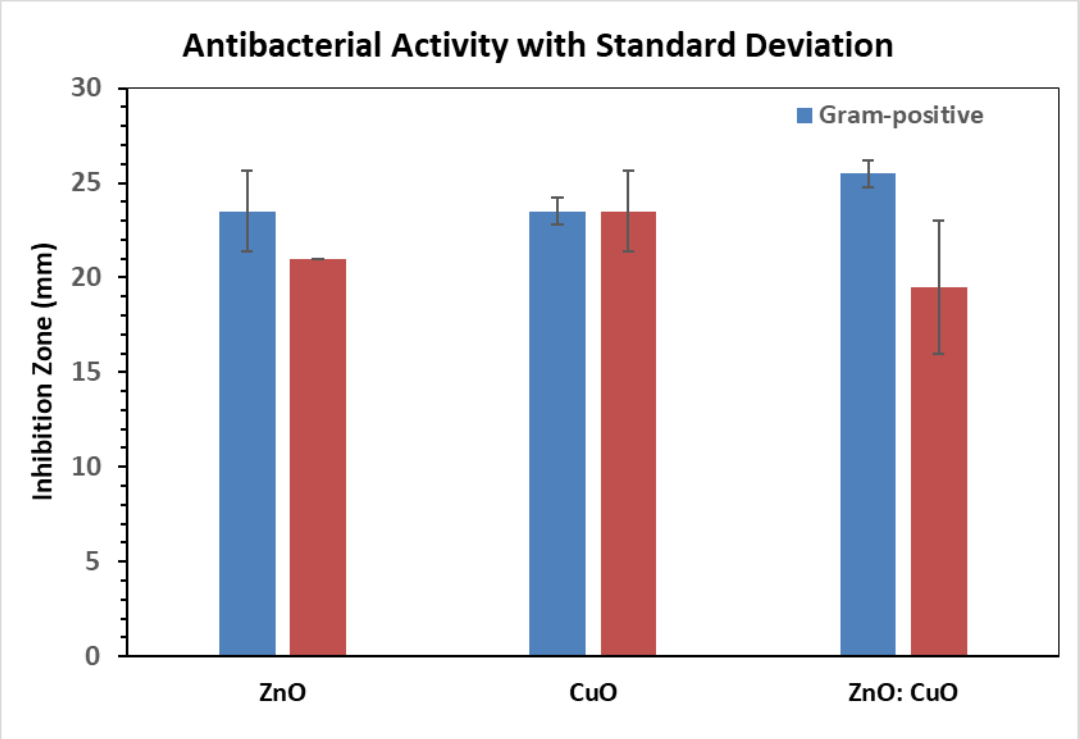

Figure 12 Antibacterial Activity of ZnO, CuO, and ZnO:CuO Nanostructures Against Gram + and Gram- Bacteria (Mean ± SD).

4. CONCLUSIONS

The laser ablation method was effectively used for the preparation of ZnO, CuO, and ZnO:CuO nanoparticles. The synthesis of nanoparticles showed excellent purity as supported by XRD, AFM, SEM, and UV-spectroscopy analyses. The composite ZnO:CuO was the most effective active antimicrobial agent against Gram-positive bacteria such as S. aureus and S. epidermidis, having an average inhibitory zone of 25.5 ± 0.71 mm and it is reported that the ZnO and CuO values are both 23.5 mm. This enhancement is likely due to the synergistic nature of ZnO and CuO, stimulating the generation of ROS as well as injuring the bacterial cell wall. Meanwhile, with respect to the bactericidal activity of Gram-negative bacteria, including E. coli and Klebsiella, CuO exhibited the greatest antibacterial activity (23.5 ± 2.12 mm) and ZnO the second highest (21.0 ± 0.00 mm). However, the activity of the ZnO:CuO composite was lower at 19.5 ± 3.54 mm.

References

[1] M. Rasheed, I. Alshalal, A. A. Rashed, M. A. Sarhan, A. S. Jaber, Indonesian Journal of Electrical Engineering and Computer Science, 33 (2024) 653. https://doi.org/10.11591/ijeecs.v33.i1.pp653-660
[2] F. Boudou, A. Guendouzi, A. Belakredar, M. RASHEED, Notulae Scientia Biologicae, 16 (2024) 13837. https://doi.org/10.55779/nsb16211837
[3] F. Boudou, A. Belakredar, A. Berkane, M. RASHEED, Notulae Scientia Biologicae, 17 (2025) 12183. https://doi.org/10.55779/nsb17212183
[4] K. K. Khudair, F. Boudou, A. Mohammed, A. Sehmi, A. Belakredar, M. S. Ibrahim, Experimental and Theoretical NANOTECHNOLOGY, 10 (2026) 869. https://doi.org/10.56053/10.S.869

[5] A. R. J. Katae, H. H. Hussein, A. S. Jaber, M. A. Sarhan, M. RASHEED, Experimental and Theoretical NANOTECHNOLOGY, 10 (2026) 725. https://doi.org/10.56053/10.2.725
[6] A. R. J. Katae, H. H. Hussein, A. S. Jaber, M. A. Sarhan, M. RASHEED, Experimental and Theoretical NANOTECHNOLOGY, 10 (2026) 795. https://doi.org/10.56053/10.2.795
[7] I. M. Mohammed, M. Rasheed, AIP Conference Proceedings, 3321 (2025) 020026. https://doi.org/10.1063/5.0289719
[8] M. Enneffati, M. Rasheed, B. Louati, K. Guidara, R. Barillé, Optical and Quantum Electronics, 51 (2019) 1. https://doi.org/10.1007/s11082-019-2015-5
[9] M. S. Ibrahim, T. T. Issa, B. Yaqoob, E. N. Fayyadh, A. Rashid, R. S. Mahmood, Experimental and Theoretical NANOTECHNOLOGY, 10 (2026) 887. https://doi.org/10.56053/10.S.887
[10] H. K. Aity, M. Rasheed, E. Dhahri, A. A. Hateef, T. Saidani, Journal of Materials Science, 61 (2026) 6226. https://doi.org/10.1007/s10853-026-12241-w
[11] A. Khaleefah, M. RASHEED, Experimental and Theoretical NANOTECHNOLOGY, 10 (2026) 289. https://doi.org/10.56053/10.s.289
[12] A. I. A. Ali, M. RASHEED, Experimental and Theoretical NANOTECHNOLOGY, 10 (2026) 277. https://doi.org/10.56053/10.s.277
[13] A. I. A. Ali, M. RASHEED, Experimental and Theoretical NANOTECHNOLOGY, 10 (2026) 239. https://doi.org/10.56053/10.s.239
[14] M. Rasheed, M. N. Mohammedali, F. A. Sadiq, M. A. Sarhan, T. Saidani, Journal of Optics, 54 (2024) 1. https://doi.org/10.1007/s12596-024-01928-5
[15] H. M. I. Al-Zuhairi, I. Alshalal, H. H. Abbood, M. Al Nuaimi, Experimental and Theoretical NANOTECHNOLOGY, 10 (2026) 855. https://doi.org/10.56053/10.S.855
[16] H. M. I. Al-Zuhairi, I. Alshalal, H. H. Abbood, M. Al Nuaimi, Experimental and Theoretical NANOTECHNOLOGY, 10 (2026) 1093. https://doi.org/10.56053/10.S.1093
[17] S. S. Batros, M. Rasheed, H. K. Aity, A. A. Hatef, T. Saidani, Materials Chemistry and Physics, 355 (2026) 132243. https://doi.org/10.1016/j.matchemphys.2026.132243
[18] Z. S. Ahmed, M. RASHEED, H. S. Ahmed, Experimental and Theoretical NANOTECHNOLOGY, 10 (2026) 329. https://doi.org/10.56053/10.s.329
[19] Z. S. Ahmed, M. RASHEED, H. S. Ahmed, Experimental and Theoretical NANOTECHNOLOGY, 10 (2026) 343. https://doi.org/10.56053/10.s.343
[20] A. Zubaidi, L. M. Asaad, I. Alshalal, M. Rasheed, Journal of the Mechanical Behavior of Materials, 32 (2023) 1. https://doi.org/10.1515/jmbm-2022-0302
[21] T. Saidani, M. Rasheed, I. Alshalal, A. A. Rashed, M. A. Sarhan, R. Barillé, Research on Engineering Structures and Materials, 9 (2023) 1. https://doi.org/10.17515/resm2023.21ma0922rs
[22] M. Rasheed, et al., Journal of Advanced Biotechnology and Experimental Therapeutics, 6 (2023) 495. https://doi.org/10.5455/jabet.2023.d144
[23] E. Kadri, et al., Journal of Alloys and Compounds, 705 (2017) 708. https://doi.org/10.1016/j.jallcom.2017.02.117
[24] M. Rasheed, R. Barillé, Journal of Alloys and Compounds, 728 (2017) 1186. https://doi.org/10.1016/j.jallcom.2017.09.084
[25] R. S. Mahmood, et al., Journal of the Mechanical Behavior of Materials, 34 (2025) 1. https://doi.org/10.1515/jmbm-2025-0040
[26] M. Enneffati, B. Louati, K. Guidara, M. Rasheed, R. Barillé, Journal of Materials Science: Materials in Electronics, 29 (2018) 171. https://doi.org/10.1007/s10854-017-7901-7
[27] F. Dkhilalli, S. Megdiche, K. Guidara, M. Rasheed, R. Barillé, M. Megdiche, Ionics, 24 (2018) 169. https://doi.org/10.1007/s11581-017-2193-8
[28] A. Keziz, M. Rasheed, M. Heraiz, F. Sahnoune, A. Latif, Ceramics International, 49 (2023) 37423. https://doi.org/10.1016/j.ceramint.2023.09.068

Exp. Theo. NANOTECHNOLOGY 10 (2026) 1365-1378
[29] F. Boudou, A. E. Sabar, M. I. Majeed, A. M. Ibraham, R. Jamal, A. Rashid, A. Belakredar, M. Bendahmane-Salmi, M. RASHEED, R. RASHEED, T. Saidani, H. D. Al-Bahadli, Experimental and Theoretical NANOTECHNOLOGY, 10 (2026) 821. https://doi.org/10.56053/10.S.821
[30] D. Kherifi, A. Keziz, M. Rasheed, A. Oueslati, Ceramics International, 50 (2024) 1. https://doi.org/10.1016/j.ceramint.2024.05.317
[31] A. J. Hussein, M. N. Al-Darraji, M. Rasheed, M. A. Sarhan, IOP Conference Series: Earth and Environmental Science, 1262 (2023) 022005. https://doi.org/10.1088/1755-1315/1262/2/022005
[32] H. K. Aity, E. Dhahri, M. Rasheed, Ceramics International, 50 (2024) 54666. https://doi.org/10.1016/j.ceramint.2024.10.324
[33] W. Saidi, N. Hfaidh, M. Rasheed, M. Girtan, A. Megriche, M. El Maaoui, RSC Advances, 6 (2016) 68819. https://doi.org/10.1039/c6ra15060h
[34] M. Rasheed, A. Khaleefah, Materials Chemistry and Physics, 355 (2026) 132112. https://doi.org/10.1016/j.matchemphys.2026.132112
[35] G. E. Alkinani, A. R. J. Katae, M. RASHEED, Experimental and Theoretical NANOTECHNOLOGY, 10 (2026) 1027. https://doi.org/10.56053/10.S.1027
[36] A. A. Hateef, E. Dhahri, M. Rasheed, H. Kadhim, Z. Abbas, N. Hassan, Physics and Chemistry of Solid State, 25 (2024) 801. https://doi.org/10.15330/pcss.25.4.801-810
[37] F. Boudou, et al., Notulae Scientia Biologicae, 17 (2025) 12593. https://doi.org/10.55779/nsb17312593
[38] A. Aukštuolis, et al., Proceedings of the Romanian Academy Series A: Mathematics, Physics, Technical Sciences, Information Science, 18 (2017) 34. https://hal.archives-ouvertes.fr/hal-02443179
[39] A. Raghdi, M. Heraiz, M. Rasheed, A. Keziz, Journal of the Indian Chemical Society, 101 (2024) 101413. https://doi.org/10.1016/j.jics.2024.101413
[40] A. Jaber, M. Ismael, T. Rashid, M. A. Sarhan, M. Rasheed, I. M. Sala, Eureka: Physics and Engineering, 4 (2023) 29. https://doi.org/10.21303/2461-4262.2023.002770
[41] E. Kadri, M. Krichen, R. Mohammed, A. Zouari, K. Khirouni, Optical and Quantum Electronics, 48 (2016) 1. https://doi.org/10.1007/s11082-016-0812-7
[42] T. Rashid, M. M. Mokji, M. Rasheed, Journal of the Mechanical Behavior of Materials, 34 (2025) 1. https://doi.org/10.1515/jmbm-2025-0074
[43] T. Rashid, M. M. Mokji, M. Rasheed, Journal of Optics, 53 (2024) 1. https://doi.org/10.1007/s12596-024-02080-w
[44] A. J. Hussein, M. N. Al-Darraji, M. Rasheed, IOP Conference Series: Earth and Environmental Science, 1262 (2023) 022007. https://doi.org/10.1088/1755-1315/1262/2/022007
[45] A. A. Abdulrahman, M. Rasheed, S. Shihab, Journal of Physics: Conference Series, 1879 (2021) 022118. https://doi.org/10.1088/1742-6596/1879/2/022118
[46] T. Saidani, M. Zaabat, M. S. Aida, R. Barillé, M. Rasheed, Y. Almohamed, Journal of Materials Science: Materials in Electronics, 28 (2017) 9252. https://doi.org/10.1007/s10854-017-6660-9
[47] M. Rasheed, O. Y. Mohammed, S. Shihab, A. Al-Adili, Journal of Physics: Conference Series, 1795 (2021) 012042. https://doi.org/10.1088/1742-6596/1795/1/012042
[48] E. Arif, R. Jamal, M. RASHEED, Experimental and Theoretical NANOTECHNOLOGY, 10 (2026) 453. https://doi.org/10.56053/10.2.453
[49] T. Saidani, S. Mokhtari, M. Rasheed, H. Lahmar, M. Trari, Journal of the Indian Chemical Society, 103 (2026) 102499. https://doi.org/10.1016/j.jics.2026.102499
[50] M. Rasheed, S. Shihab, O. Alabdali, A. Rashid, T. Rashid, Journal of Physics: Conference Series, 1999 (2021) 012077. https://doi.org/10.1088/1742-6596/1999/1/012077

Exp. Theo. NANOTECHNOLOGY 10 (2026) 1365-1378